

THE UNIVERSITY OF MICHIGAN

COLLEGE OF ENGINEERING  
Department of Chemical and Metallurgical Engineering  
Department of Mechanical Engineering

INVESTIGATION OF LIQUID METAL  
BOILING HEAT TRANSFER

Richard E. Balzhiser  
Project Director

Bruce F. Caswell                      Robert E. Barry  
Andrew Padilla, Jr.                  Robert L. Gahman  
   Herman Merte, Jr.

ORA Project 05750

under contract with:

FLIGHT ACCESSORIES LABORATORY  
AERONAUTICAL SYSTEMS DIVISION  
AIR FORCE SYSTEMS COMMAND  
UNITED STATES AIR FORCE  
WRIGHT-PATTERSON AIR FORCE BASE, OHIO  
CONTRACT NO. AF 33(657)-11548

administered through:

OFFICE OF RESEARCH ADMINISTRATION    ANN ARBOR

August 1965

"To expedite dissemination of information, this report is being forwarded for your information prior to review and approval by the ASD project officer and is, therefore, subject to change. Any comments which you may have should be forwarded to ASD (Mr. Charles L. Delaney), Wright-Patterson AFB, Ohio, within 15 days of receipt to insure correction of errors before final approval is given.

enqn  
UMR 0522  
(v. 11)

## FOREWORD

This report summarizes progress on Contract AF 33(657)-11548 from May 1965 through August 1965. This contract provides for the continuation of the experimental programs initiated under the original contract between the University of Michigan and Aeronautical Systems Division. Investigation is being conducted in the Liquid Metals Laboratory of the Department of Chemical and Metallurgical Engineering at the University of Michigan. Professor Richard E. Balzhiser is serving as Project Director and Messrs. Barry, Caswell, Padilla and Gahman, all graduate students in Chemical Engineering have contributed to specific portions of the program. Mr. Charles L. Delaney and Lt. Ronald L. Bane have provided technical liaison with Aeronautical Systems Division.

## ABSTRACT

Critical heat flux determinations with rubidium have continued during this period. These burnout results along with other liquid metal burnout data have been correlated with the following dimensionless relation:

$$(q/A)_c = 1.02 \times 10^{-6} \frac{\lambda^2 \rho_v k}{C_p \sigma} \left( \frac{\rho_l - \rho_v}{\rho_v} \right)^{0.65} Pr^{0.71}$$

The charging of cesium has been completed and burnout determinations are about to commence.

A film boiler has been operated during this period and has yielded data over pressure range of 2 - 19mm mercury. The data obtained falls slightly above the predictions of Berenson for potassium film boiling at a pressure of a 0.1 atm. Data obtained for which the surface temperature exceeded the saturation temperature by greater than 700°F yielded reasonably consistent results when the flux was calculated by two independent procedures. At lower values of the surface temperature, unusual behavior was encountered which is probably related to transitional effects which began to occur on the wall of the vessel near the boiling plate. Studies currently underway are expected to yield further information on this phenomenon. For values of  $T_{surf} - T_{sat}$  from 700 - 900°F and over the pressure range of 2 - 19mm of mercury, the heat fluxes obtained ranged from 4,000 to 8,000 BTU/(hr.)(sq. ft.).

During the last quarter a forced circulation apparatus was operated to yield condensing coefficients for sodium over a temperature range of

1240°F to 1525°F and a range of heat fluxes from 215,000 to 583,000 BTU/(hr.)(sq. ft.). The condensing coefficient was observed to be essentially constant over these ranges at a value of  $10,800 \pm 3,300$  BTU/(hr.)(sq. ft.)(°F).

Two phase flow studies including both heat transfer and pressure drop results were accomplished. Thirty-eight data points were obtained with qualities ranging up to 24% in the flowing potassium system. The results of these studies are presently being processed to yield heat transfer coefficients to two phase flowing potassium.

## TABLE OF CONTENTS

POOL BOILING STUDIES . . . . .	1
Rubidium Burnout Results. . . . .	1
Cesium Burnout Studies. . . . .	6
Correlation of Burnout Results. . . . .	8
FILM BOILING . . . . .	14
Description of Experimental System. . . . .	14
Method of Charging. . . . .	19
Operation . . . . .	19
Analysis of Data. . . . .	20
FORCED CIRCULATION STUDIES . . . . .	31
Loop Operation. . . . .	31
Void Fraction Studies . . . . .	34
THE CONDENSATION OF SODIUM AT HIGH HEAT FLUXES . . . . .	40

## LIST OF FIGURES

### FIGURE

1. Comparison of Rubidium Burnout Data with Correlations . . .	3
2. Heater Surface Temperature. . . . .	4
3. Photo of Heater . . . . .	5
4. Summary of Alkali Metal Burnout Data. . . . .	9
5. Correlation of Alkali Metal Burnout Data. . . . .	10
6. Comparison of Sodium Burnout Data with Correlations . . . .	11
7. Correlation of Burnout Data . . . . .	13
8. Schematic Diagram of Film Boiling Apparatus . . . . .	15
9. Photograph of Boiling Plate . . . . .	17
10. Boiler and Heater Assembly. . . . .	18
11. Location of Boiling Plate Thermocouples . . . . .	22
12. Location of Thermocouples Outside Boiling Plate . . . . .	23
13. Temperature Distribution Inside of Computer Model of Boiling Plate . . . . .	25
14. Comparison Between Boiling Surface Flux and Flux Calculated from Temperature in Plate. . . . .	26
15. Film Boiling of Potassium . . . . .	29
16. Gamma-ray Source and Scintillation Crystal Holder . . . . .	35
17. Void Fraction Instrumentation . . . . .	36
18. High Voltage Characteristics. . . . .	38
19. Differential Pulse Height Spectra Multiplier 10, High Voltage 850 . . . . .	39

## POOL BOILING STUDIES

Bruce F. Caswell

The critical heat flux was measured for rubidium in saturated pool boiling on a 3/8-inch OD horizontal cylindrical heater. Thirteen data points were obtained in the pressure range 0.5 to 28 PSIA. These data agreed closely with the liquid metal burnout correlation presented in the previous report (1). A more general correlation, involving the additional factor  $Pr^{0.71}$ , was developed for both metallic and non-metallic materials.

### Rubidium Burnout Results

During the past reporting period eleven additional burnout points for rubidium were obtained in addition to the two points reported previously (1). These results are plotted in Figure 1 and compared with the burnout correlations of Noyes, Rohsenow-Griffith, Zuber-Tribus, and the author's liquid metal correlation based on sodium and potassium burnout results (1). The rubidium data follow the relation  $(q/A)_c = 314,000 p^{0.086}$  (PSIA), with a 95% confidence range of  $\pm 5\%$  and a correlation coefficient of 0.795.

The data points generally were taken in pairs in order to determine if the method used in approaching the burnout point was affecting the results. A run was made by fixing the heat flux and then slowly reducing pressure until burnout occurred, and then a second run was made by setting the pressure determined in the first run and then increasing



the heat flux to the burnout point. Five such pairs can be seen in Figure 1. It was found that the average difference between the two values in each pair was 5%.

A typical temperature record from a heater surface thermocouple made during a burnout determination is shown in Figure 2. This run was made by setting a constant heat flux and slowly decreasing the pressure until burnout occurred. As shown, at the burnout point the temperature suddenly increased by approximately 350°F. During the run there are large temperature excursions from which the heater recovers without burning out. In particular, 1 1/2 minutes before burnout occurred there was a 100°F excursion with recovery. This suggests that for heaters of small dimension the heat transfer characteristics of the heater material could have an effect on the burnout point because a thin heater or one of low thermal conductivity would not be able to recover or conduct heat away during a local excursion. Near the beginning of the run there were several excursions of 50 - 60°F.

The first two rubidium burnout points were taken at 3 PSIA and were reported previously (1). They were taken on the same heater, which failed before another run could be made. A photograph of this heater after failure is shown in Figure 3. It failed during an experimental run while attempting to obtain a point at 10 PSIA. The heater was at a temperature of 1200°F when failure occurred. It was theorized that the tube burst because of the differential thermal expansion of the graphite electrode. Two more heaters failed in a similar manner while attempting to get additional burnout data.

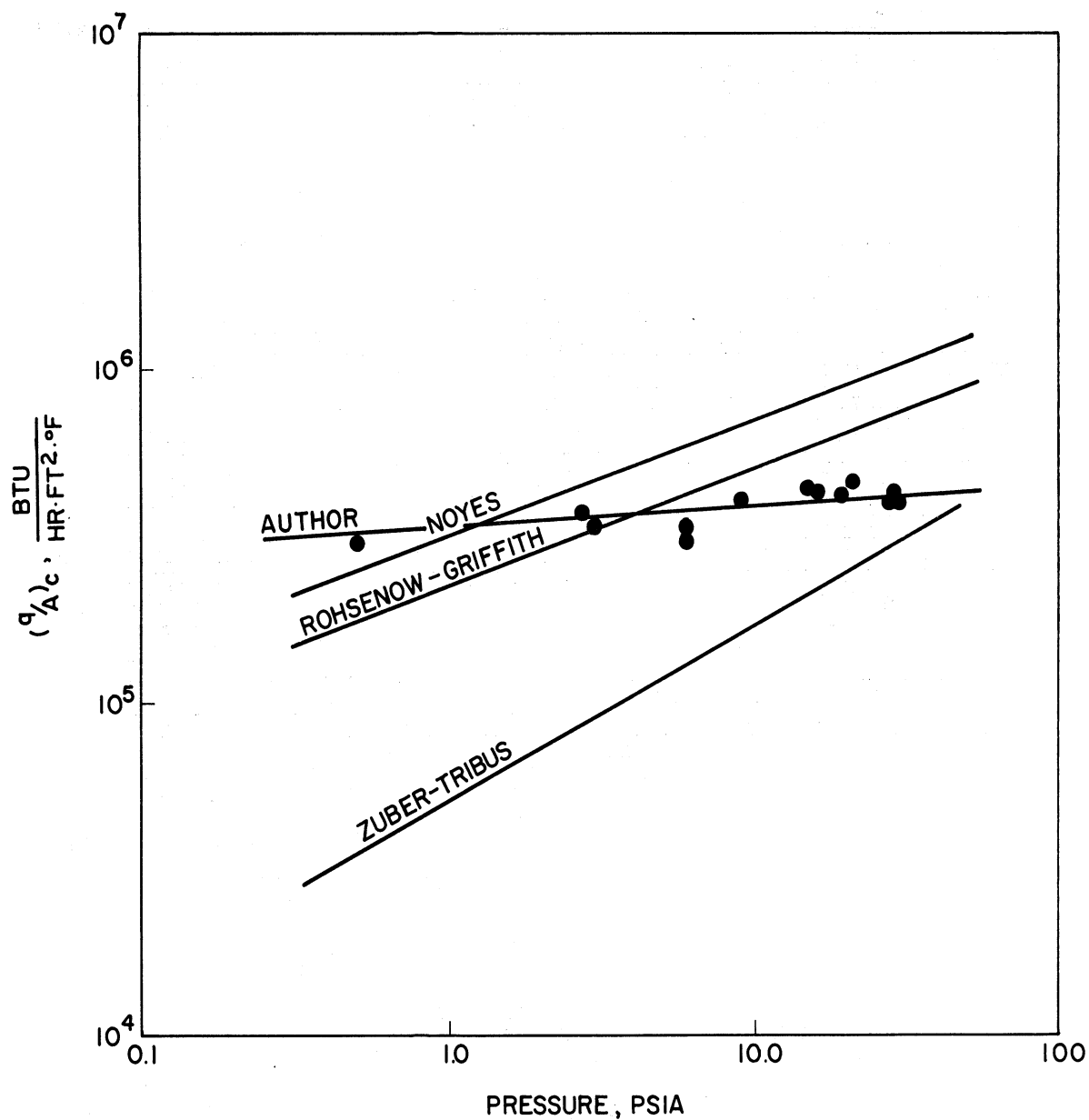


Figure 1. Comparison of rubidium burnout data with correlations

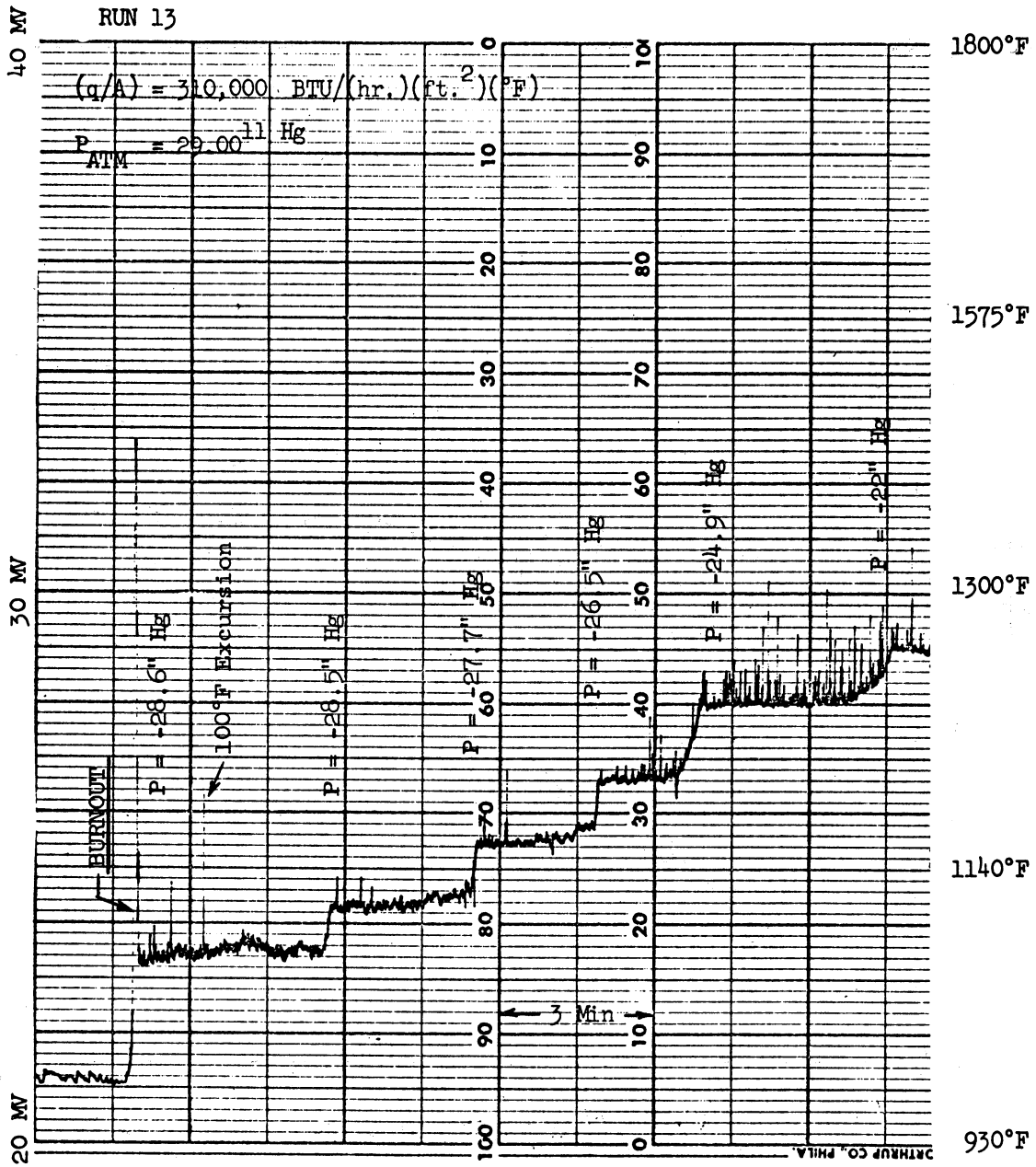
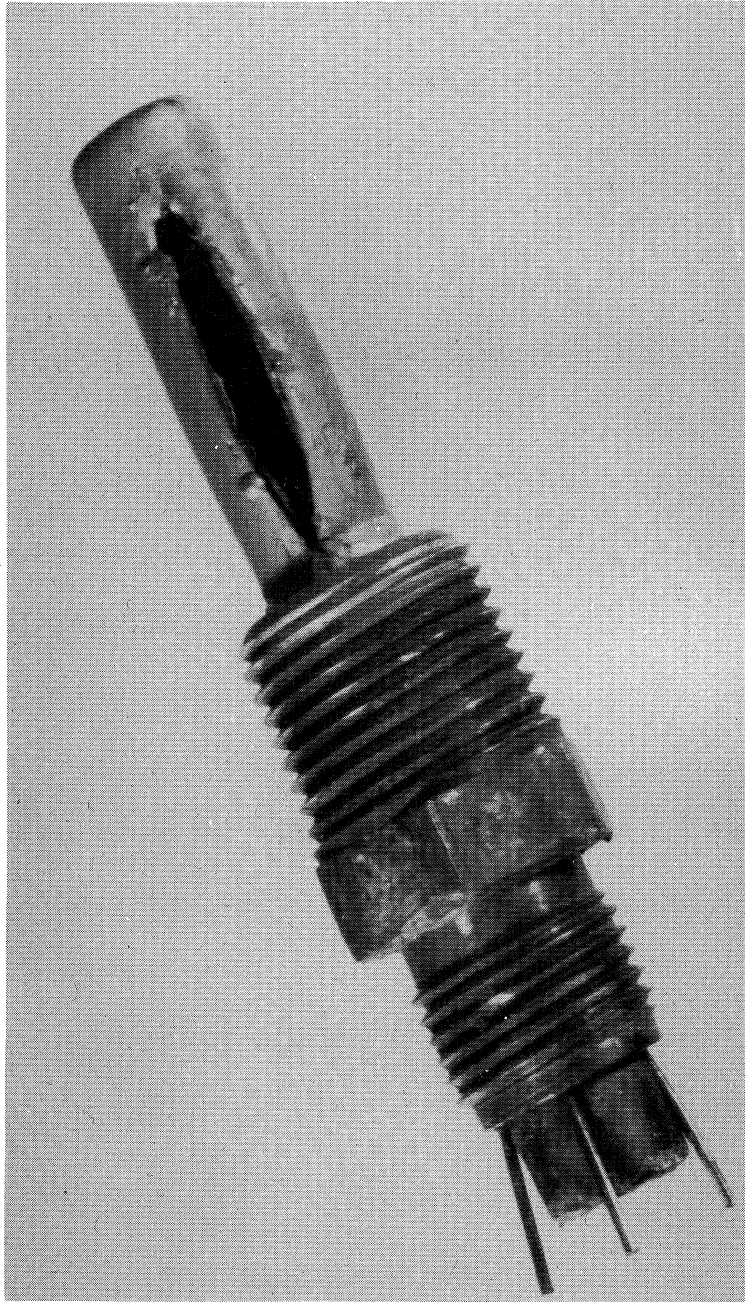


Figure 2. Heater surface temperature



**Figure 3. Photo of heater**

In order to prevent this type of failure, subsequent heaters were fabricated with 0.003 - 0.005 inches of radial clearance between the electrode and sleeve in order to allow for expansion.

In order to reduce the electrical contact resistance between the electrode and the end of the heater, those fabricated recently have a 1/32-inch diameter hole drilled through the graphite electrode lengthwise to prevent an air pocket from causing poor electrical contact between the electrode and the metal at the closed end of the heater.

With a single heater of the new design, as described above, the other eleven data points were obtained. This heater then had to be replaced because all three of the surface thermocouples failed and then broke off inside the wells when an attempt was made to remove them. This heater was otherwise in good condition, except that some of the Microbrazed, used to seal the thermowells onto the surface, had been corroded or dissolved away. Another heater was installed but during the first run the boron nitride insulating sleeve cracked and the heater shorted out. It was then decided to dump the rubidium from the equipment and commence work on cesium.

#### Cesium Burnout Studies

Before cesium could be loaded to the pool boiler, some cleaning and modification of the equipment was done. The rubidium metal was drained at 175°F into an open pail. No fire occurred during this operation although there was some smoldering. The rubidium was discarded.

All connections to the equipment were removed, the heater was removed, and the equipment was left for one week to slowly react with the

ambient air. During this period there was some drainage of burning metal from the bottom connection. The next step was to introduce small amounts of methanol and then water into the equipment. Finally, the equipment was cleaned with 36% HCl and then water. It was then steamed out for three days. It was then reconnected to the various vacuum and inert gas lines and heated and evacuated for several days.

During the rubidium experiments the Hoke bellows-sealed valve in the charge line failed. In attempting to drain through it, it was found to be frozen in the closed position. It was cut off and replaced with a similar valve of the positive return type. Another was installed in the line leading up to the storage vessel above the top flange. This is necessary for the cesium work because with its low melting point of 80°F there would be difficulty in keeping it frozen in the storage vessel as was done with potassium, sodium, and rubidium.

Three of the thermocouples on the outside wall of the boiling vessel opened at the junction during the rubidium work and were repaired. All of the nine wall thermocouples were repositioned so as to be in direct contact with the wall. The same locations as described previously were used for the thermocouples.

Two of the five guard heaters developed open circuits during the rubidium work. It was found, upon examination, that all of the guard heater elements had become badly oxidized and were extremely brittle. These elements had been specified by the manufacturer, the Hevi-Duty Electric Company, to be operable to 2200°F. In this work they were never operated above 1600°F and were always in vacuum or an inert gas atmosphere. All five of the heater elements were replaced using the same locations as before.

Two pounds of cesium of 99.9% purity were purchased from the MSA Research Corporation. They specify that the principal impurity is rubidium. One pound of the cesium metal was charged to the apparatus and burnout studies will commence shortly.

Figure 4 shows the predicted values of the critical flux for cesium using the author's liquid metal burnout correlation in Figure 5.

#### Correlation of Burnout Results

Figure 6 is a comparison of the sodium results reported previously with the burnout correlations of Noyes, Rohsenow-Griffith, Zuber-Tribus, and the author's liquid metal correlation. Regression analysis was performed on the sodium and rubidium data and also on the potassium data reported previously. The results of this analysis are tabulated below:

<u>Material</u>	<u>Regression Equation</u>	<u>95% Confidence Range</u>	<u>Correlation Coefficient</u>
Potassium	$(q/A)_c = 415,00 p^{0.167}$	$\pm 3.3\%$	0.971
Rubidium	$(q/A)_c = 314,00 p^{0.086}$	$\pm 5 \%$	0.795
Sodium	$(q/A)_c = 505,00 p^{0.182}$	$\pm 7 \%$	0.809

The liquid metal correlation of the above data shown in Figure 5 has a 95% confidence range of  $\pm 6\%$  and a correlation coefficient of 0.972.

This indicates that the correlation has approximately the same amount of scatter about it as the data on each liquid metal plotted individually against pressure, a very surprising result. Some caution should be exercised in applying the liquid metal correlation to systems other than

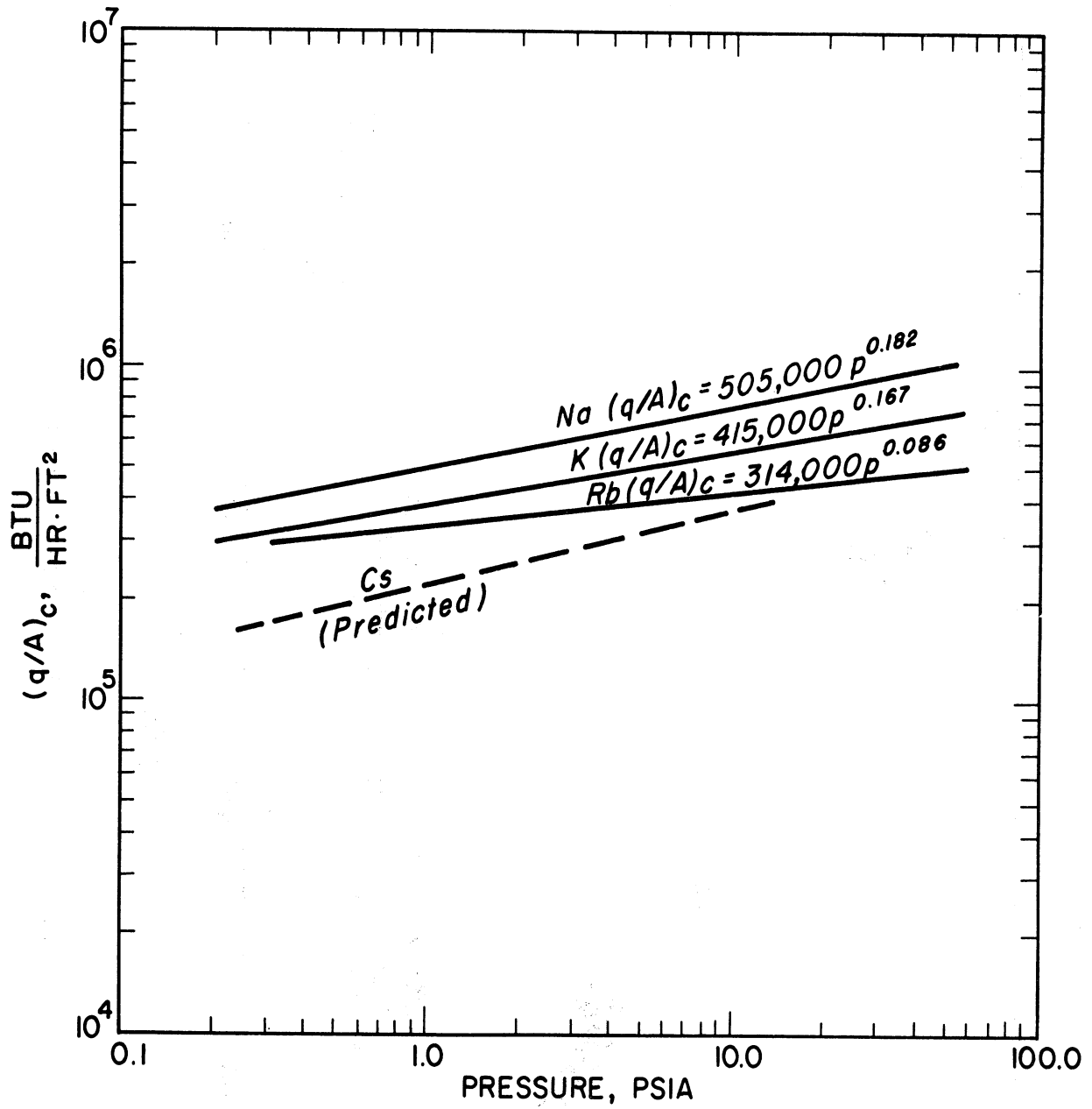


Figure 4. Summary of alkali metal burnout data



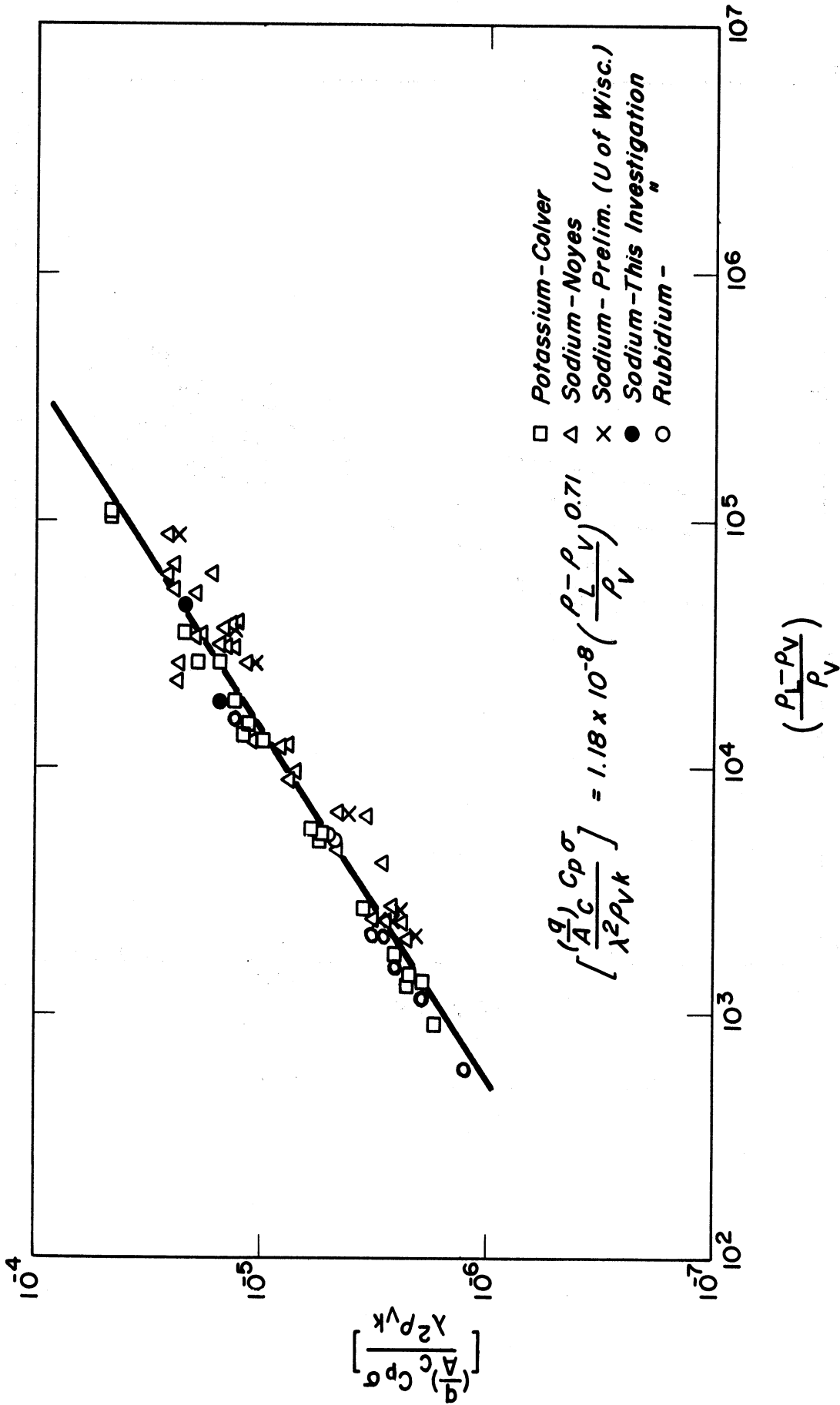


Figure 5. Correlation of alkali metal burnout data

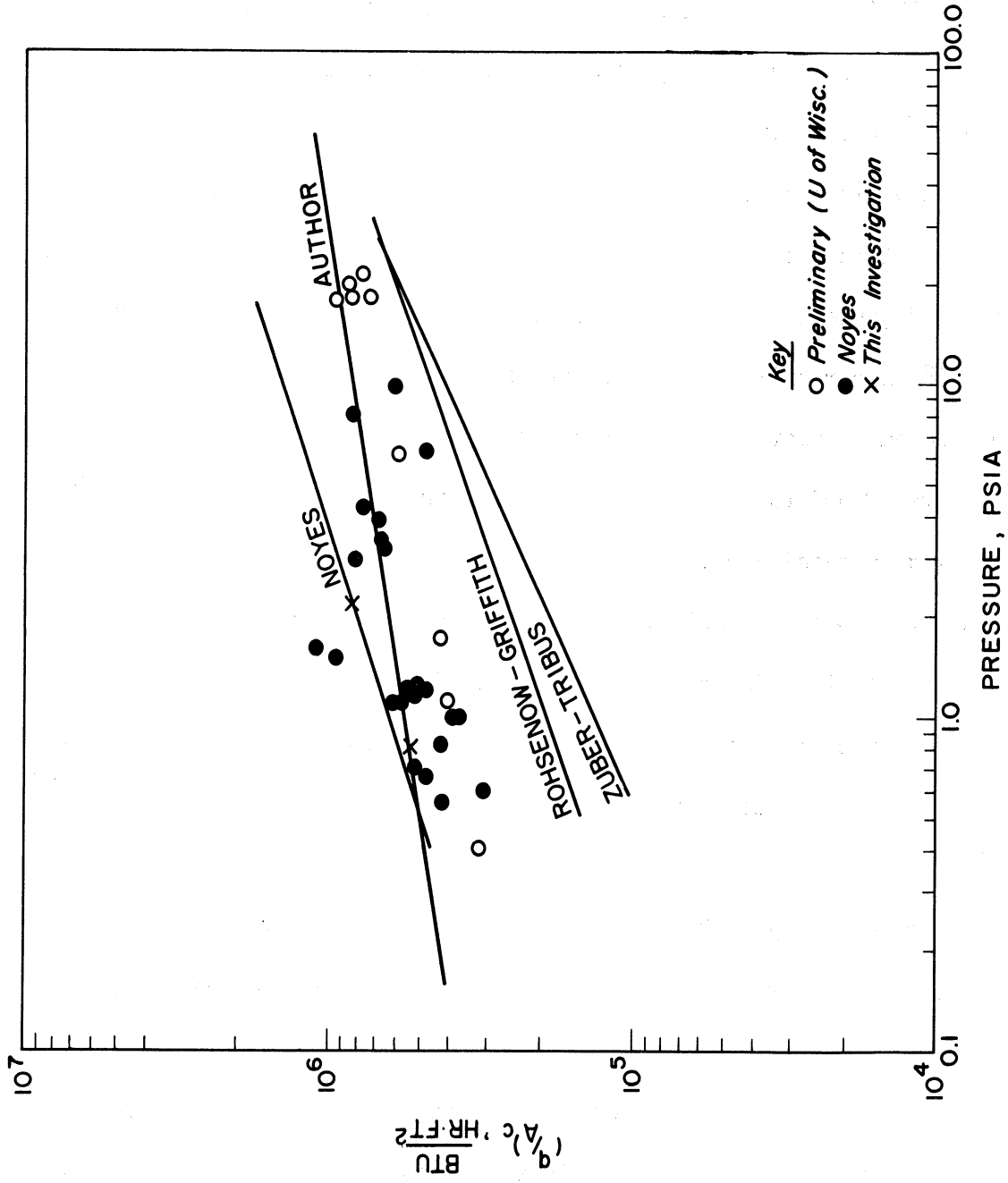


Figure 6. Comparison of sodium burnout data with correlations

those used in obtaining the data. All of the liquid metal results have been obtained on horizontally mounted cylindrical heaters of 1/4-inch to 1/2-inch OD and all of the data were obtained in the low pressure range, below 40 PSIA. It is possible that for other geometries or higher pressures, significant deviations from the correlation might occur. In particular, very thin heaters or those made from low conductivity materials would tend to give lower results of the critical heat flux.

It is interesting to note that the correlation predicts the correct pressure dependence for each material even though this dependence varies from 0.086 for rubidium to 0.182 for sodium. Most of the other correlations investigated predict the same pressure dependence for every material.

It was found that the introduction of the additional factor,  $Pr^{-0.71}$ , to the liquid metal correlation resulted in a more general relation which gave a fit of both metallic and non-metallic burnout results. This general correlation is shown in Figure 7. In this correlation 82 data points were used of which 60 were liquid metal points. The 95% confidence range about the correlation is  $\pm 16\%$  and the correlation coefficient is 0.831.

It is necessary to keep in mind that there may be a geometry effect which is not considered here. Also, there might be deviations from this correlation at pressures near the critical pressure. As with all correlations, the values of the physical properties used in the computation are not always accurately known. This is probably more true in the case of the liquid metals.

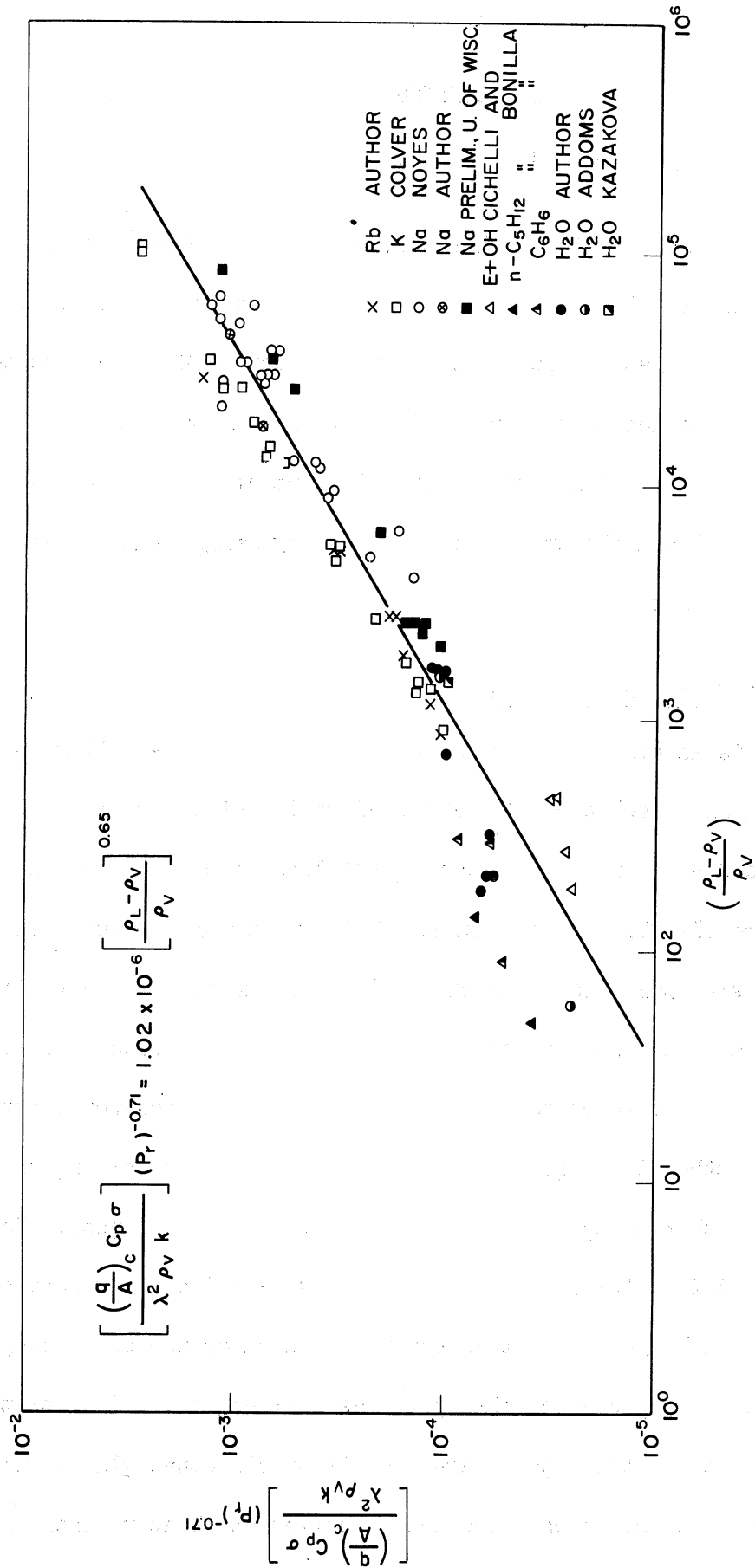


Figure 7. Correlation of burnout data

## FILM BOILING

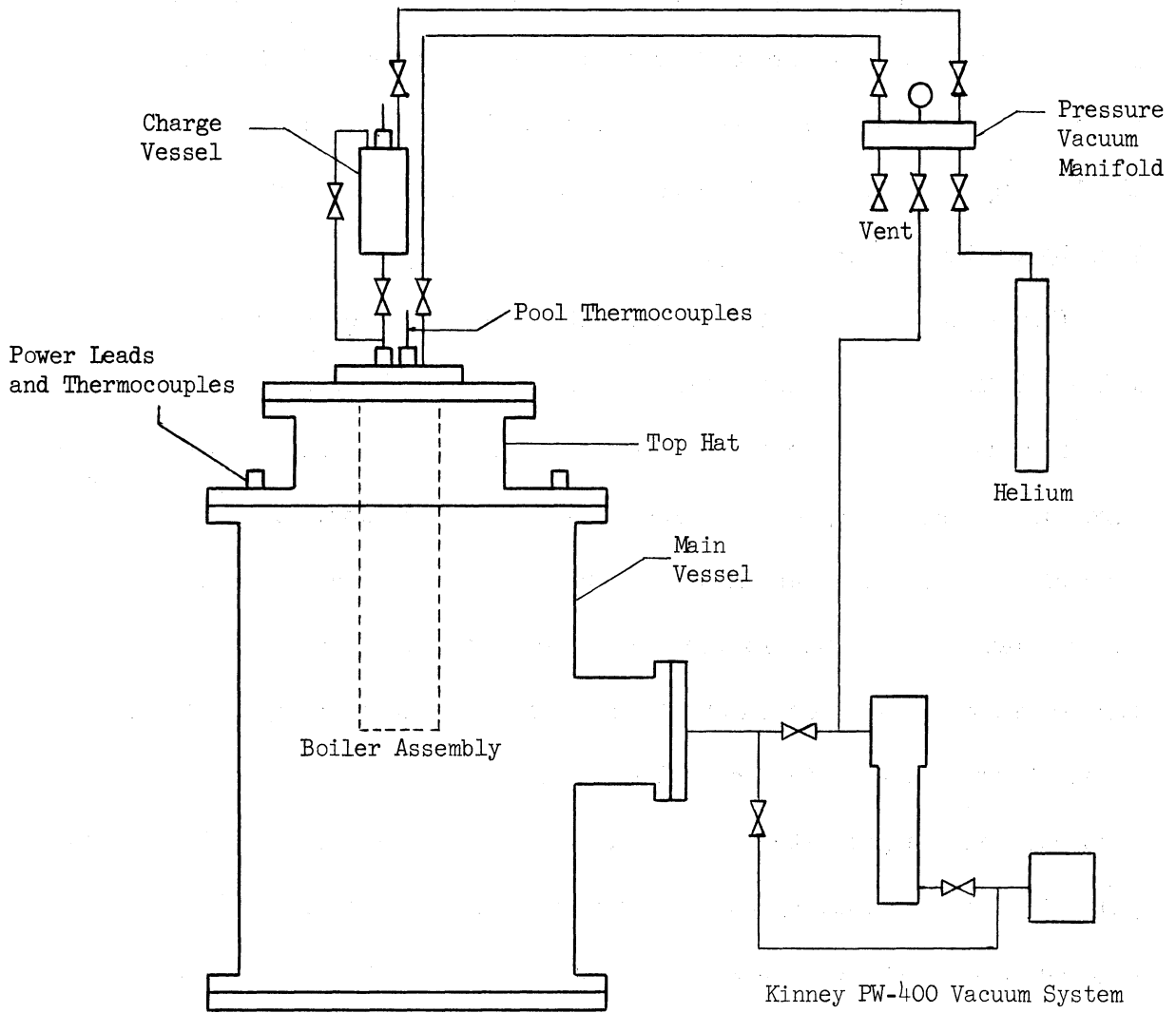
Andrew Padilla, Jr.

The 3-inch diameter film boiler previously proposed (2) consisted of a 3 1/2-inch diameter Mo-0.5 Ti block joined to a Haynes-25 pipe. Several attempts at vacuum brazing the Mo-0.5 Ti to the Haynes-25 were unsuccessful and have led to the design and fabrication of an all stainless steel assembly. Data for the film boiling of potassium at reduced pressures have been obtained and the apparatus is currently being readied for operation at higher pressures.

### Description of Experimental System

Figure 8 is an overall schematic diagram of the film-boiling apparatus. The environmental vessel consists of a 21-inch diameter x 27-inch long main chamber and a 13-inch diameter x 6-inch long upper section. The main chamber is directly flanged to a Kinney PW400 vacuum system consisting of a 4-inch diffusion pump and a Welsch Duo-Seal vacuum pump. The filling line from the charge vessel enters the boiling chamber through a Conax gland which allows it to be raised for charging and lowered for emptying the boiler. Another Conax gland at the top flange of the boiling chamber allows for four thermocouples to be lowered into the liquid pool. The filling line and four thermocouples pass through a 3-inch long scrubbing section packed with stainless steel shavings and enter the condensing portion of the boiling chamber through holes drilled in the drip plate. The bottom section of the upper chamber contains six Conax glands for power leads and thermocouples. The entire boiler and heater assembly is

Figure 8. Schematic Diagram of Film Boiling Apparatus



inserted into the vessel through an opening in the top flange.

A photograph of the boiling plate is shown in Figure 9. The boiling plate was machined from solid bar stock 3 1/2-inch diameter x 1 1/2-inch long. The plate section is 0.504-inch thick and contains six 1/16-inch diameter holes at two different depths below the boiling surface and three different radii from the center. The thin-walled section above the boiling plate is .050-inch thick and is designed to reduce the heat loss by conduction from the plate.

Figure 10 is a detail of the boiling plate and heater assembly. A 1/16-inch OD x 55-inch long swaged heater has been Microbrazed to the .050-inch wall of the boiling plate. This heater consists of two Nichrome wires insulated by magnesium oxide in an Inconel sheath. The heater assembly consists of a graphite heater with Lava insulators above and below. Lava is hydrous aluminum silicate which had been cured at 1850°F for 30 minutes. Molybdenum shunts are forced against the graphite by means of springs to maintain good electrical contact. Good thermal contact between the graphite heater, the top Lava insulator, and the boiling plate is also obtained by using a spring. The springs are compressed by tightening down on three tie rods connecting the compression plate and the drip plate above the condenser.

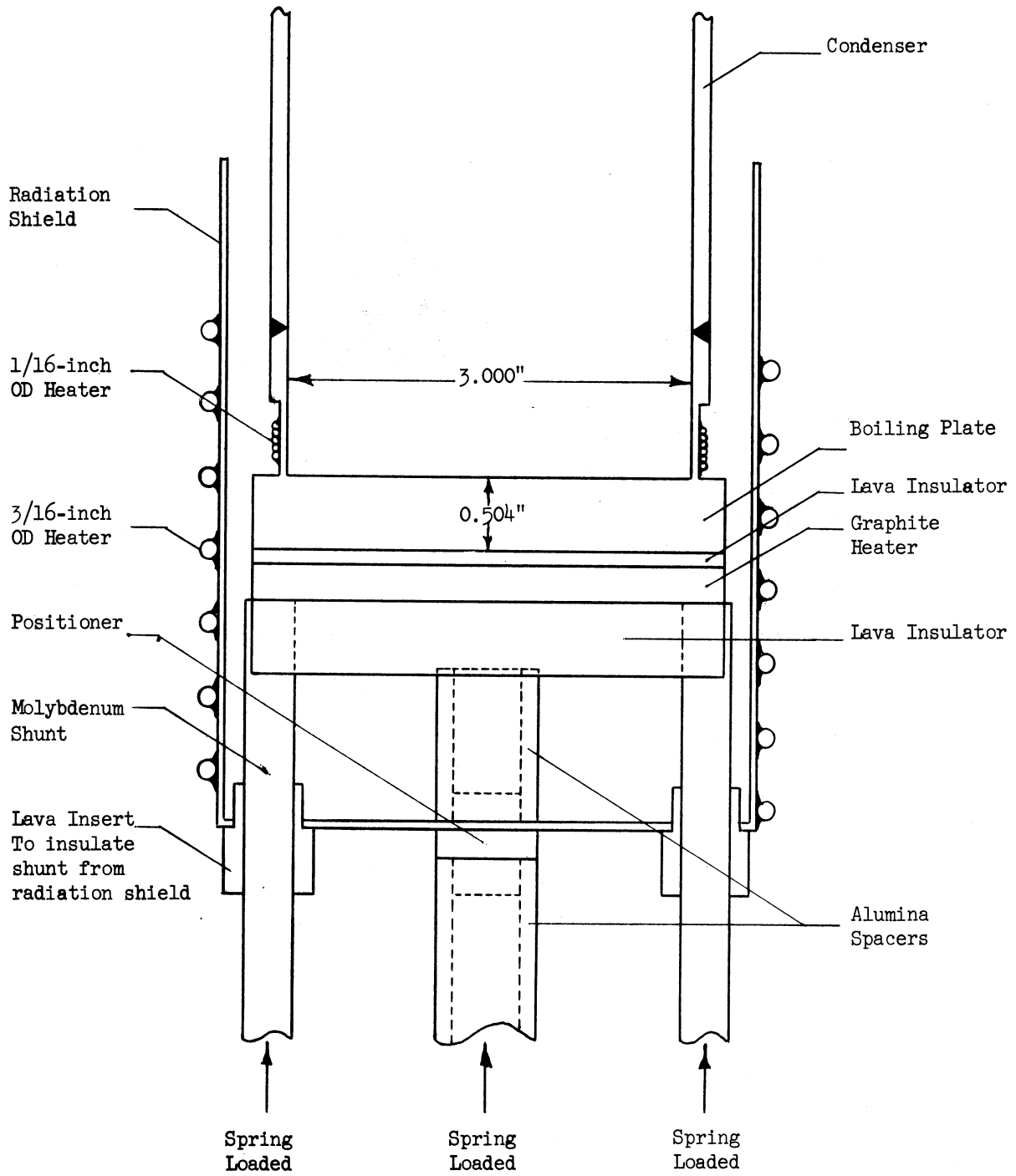
The heater assembly and boiling plate are completely surrounded by a 4-inch OD radiation shield to which is Microbrazed a 3/16-inch OD x 93-inch long swaged heater similar to the one on the wall of the boiling plate. Holes on the side and bottom of the shield allow for the boiling plate thermocouples and molybdenum shunts respectively. Lava insulators keep the molybdenum shunts from contacting the bottom of the radiation shield.



Figure 9. Photograph of Boiling Plate



Figure 10. Boiler and Heater Assembly



The six boiling plate and four liquid pool thermocouples are made of Pt - Pt 13 Rh. Twelve other Chromel-Alumel thermocouples are located at various parts of the system. The Pt - Pt 13 Rh thermocouples are monitored on three Leeds and Northrup Speedomax H Compact Azar recorders and can also be read on a Leeds and Northrup No. 8662 portable precision potentiometer when steady state conditions are achieved. The Chromel-Alumel thermocouples are hooked up to a 12-point recorder.

#### Method of Charging

The boiling chamber and connecting lines were leak-checked using a helium mass spectrometer and then flushed several times with inert gas. The boiling chamber was then evacuated and the plate heated to approximately 1600°F. The charge vessel and lines were heated to 200 - 250°F with heating tapes. The valve below the charge vessel was slowly opened and the potassium allowed to drip from the fill line, which was located 3/4-inch above the boiling plate. The temperature of one of the thermocouples in the boiling plate was continuously monitored on a recorder. As the potassium slowly dripped on to the plate, the plate temperature began to drop. The power to the graphite heater was slowly increased to maintain the boiling plate at approximately 1600°F. When the increase in power input was insufficient to keep the boiling plate temperature from falling, the charge valve was turned off until the temperature could be brought back up to 1600°F. Thus it was possible to obtain film boiling without passing through nucleate boiling and the critical heat flux.

#### Operation

After film boiling was established, the temperatures in the system were continuously monitored on a slow 12-point recorder. The time required

for steady state to be reached after changing the power to the graphite heater was approximately one hour. Even after several hours of operation at the same power level, the temperatures slowly drifted in a random manner. Since the power required was very low, these fluctuations were due to changes in the line voltage of the power supply to the rectifier. This was evidenced by the fact that large fluctuations were encountered at 8 a.m. and 5 p.m. when power utilization changes drastically.

When steady state was achieved, the boiling plate temperatures were taken with a Leeds and Northrup No. 8662 portable precision potentiometer. The power to the graphite heater was then changed and the system allowed to come to steady state again. Data at several power levels was obtained at each pressure level. The pressure was increased by slowly bleeding helium into the boiling chamber or decreased by cracking the valve to the vacuum system. The data was taken on the following ranges of saturation temperatures: 684-693°F, 812-815°F, 874-878°F, and 737-745°F.

The runs were made using the graphite heater only. The 1/16-inch OD heater brazed to the .050-inch tube wall above the boiling plate had burned out during a previous start-up attempt. The 3/16-inch OD heater brazed to the radiation shield was not used since the radiation shield opposite the boiling plate was hotter than the boiling plate thereby eliminating outward radial heat losses in this section. This was due to upward conduction from that part of the radiation shield directly opposite the graphite heater. Another reason for not using the heater on the radiation shield was that the condensing capacity was reduced.

#### Analysis of Data

In the present experimental system, the heat flux at the boiling

surface must be calculated by measuring the temperature at several points in the boiling plate using thermocouples. The temperature measurements are then used with the known distance between thermocouples and the thermal conductivity to establish the heat flux across the plate. This heat flux is equal to the flux at the boiling surface only if no radial gradients exist. The plate contains thermocouples at two different depths below the boiling surface to measure the axial temperature gradient and at three different radii to detect radial gradients.

The boiling plate is connected to a tube which serves as the containment vessel for the boiling liquid. The flux lines in the boiling plate depend on the relative resistances to heat flow of the boiling surface and axial conduction up the tube wall. If the boiling coefficient is very low, as in film boiling, then the relatively low resistance to heat flow by axial conduction up the wall of the tube severely distorts the flux lines in the plate. This radial heat flow in the plate makes the axial temperature gradient an inaccurate indication of the flux occurring at the boiling surface. The relationship between the boiling surface flux and the flux calculated by measuring the axial temperature profile in the plate is quite complicated and requires the determination of the temperature field in the boiling plate.

Figure 11 is a diagram drawn to scale showing the location of the thermocouples in the boiling plate. Figure 12 shows the location of other thermocouples in the system. The temperatures recorded during operation in film boiling are noted. Based on these temperatures and using the known axial distances between thermocouples and the thermal conductivity of stainless steel type 316, the following fluxes can be calculated.

Figure 11. Location of Boiling Plate Thermocouples

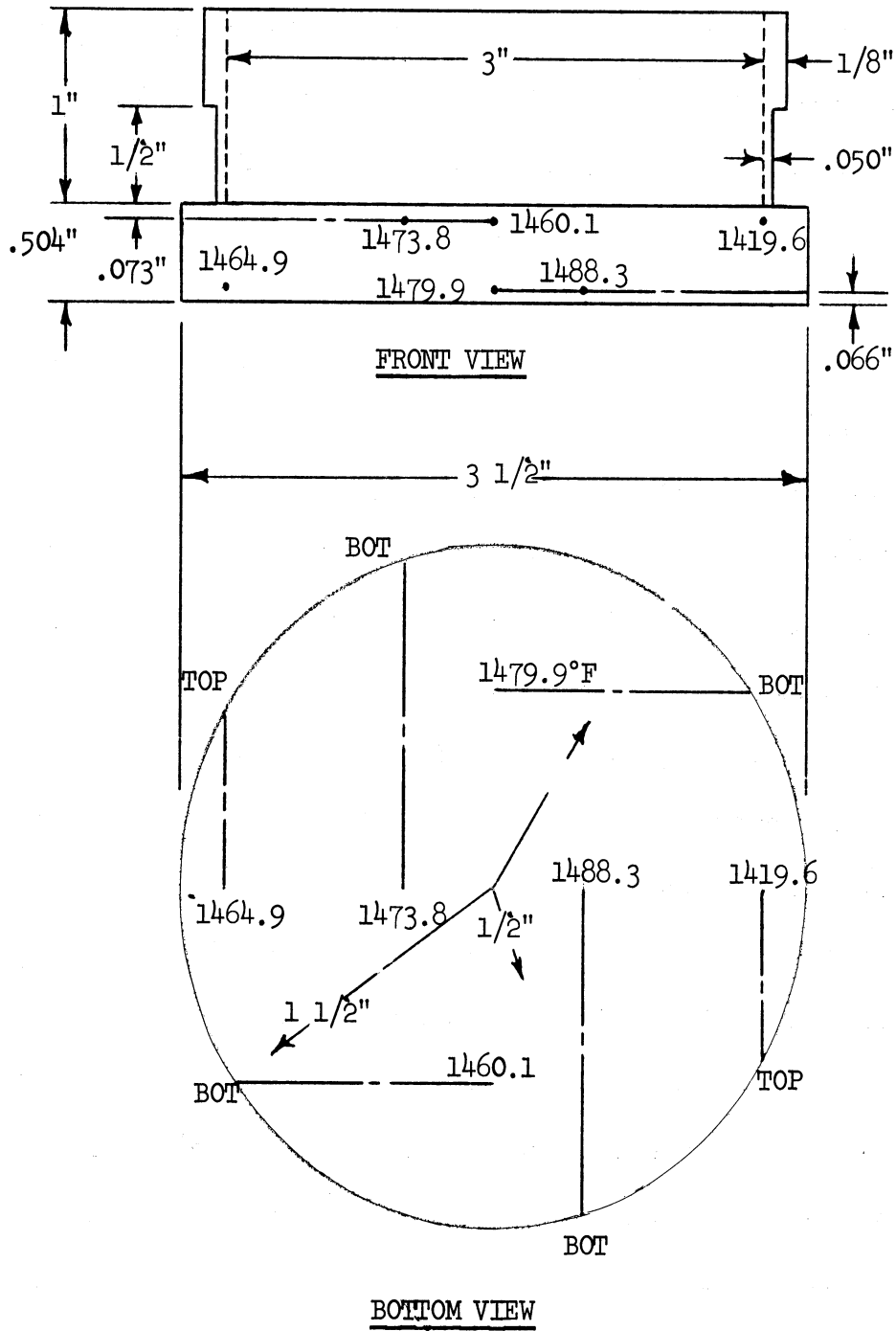
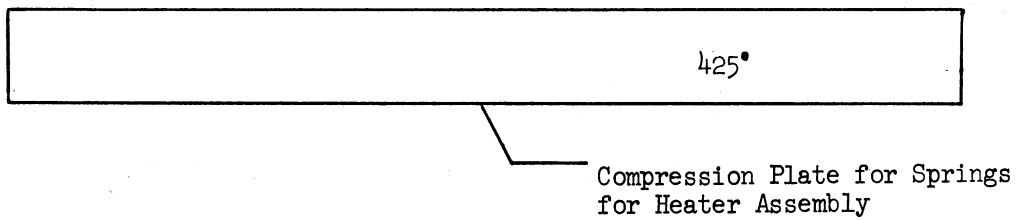
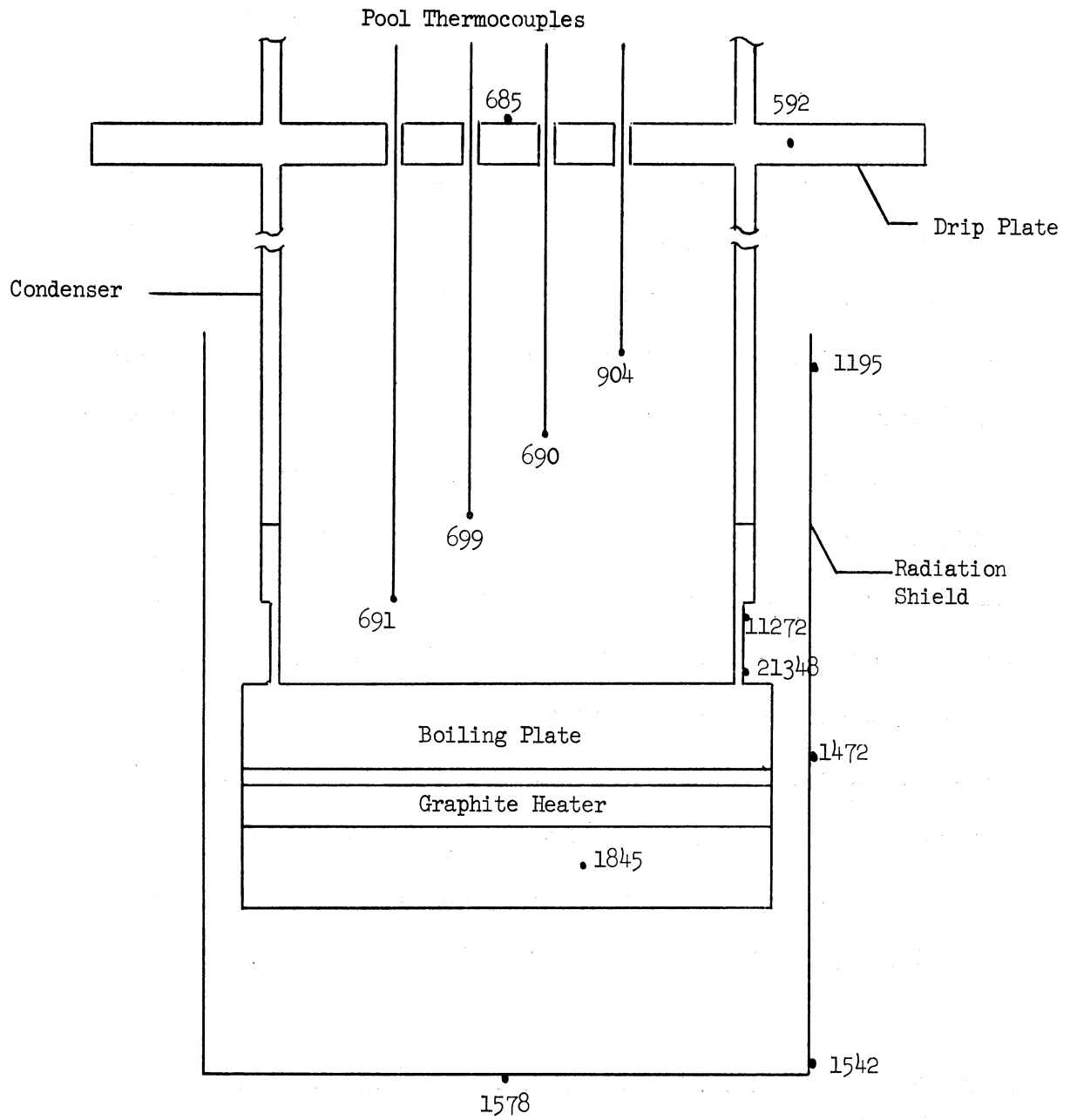


Figure 12. Location of Thermocouples Outside Boiling Plate



Radial distance from center of boiling plate	Heat flux BTU/(hr.)(sq.ft.)
1/2"	6,480
1 "	8,860
1 1/2"	19,850

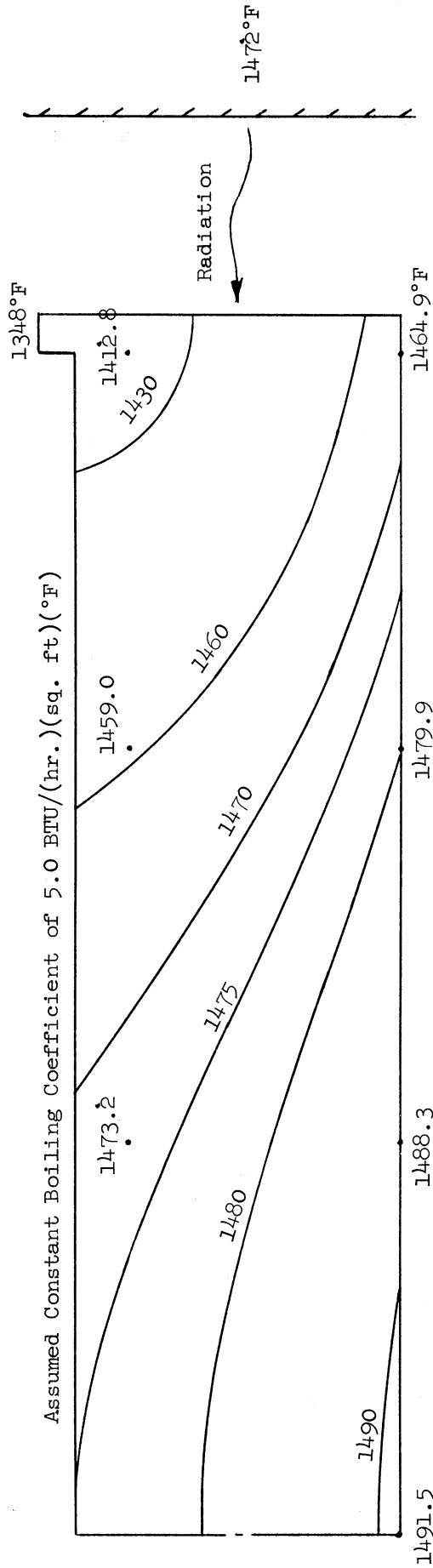
In order to determine whether these calculated fluxes actually correspond to the boiling fluxes, a computer program was developed which determines the temperature field in the boiling plate for any set of operating conditions. Laplace's equation in cylindrical coordinates with polar symmetry was used. Figure 13 shows the temperature distribution in the computer model for the boiling plate for the set of operating conditions in Figure 11. The temperatures along the top surface of the plate can be used with the assumed boiling coefficient and liquid temperature to calculate the radial variation in the boiling surface flux (BOIL). By taking the temperatures at two different depths below the boiling surface, the radial variation in the flux which can be measured by thermocouples can also be calculated (MEASRD). The distances between grid points in the computer model and the corresponding distances between thermocouples in the boiling plate are:

<u>Distance from top surface</u>	<u>1/2" radius</u>	<u>1" radius</u>	<u>1 1/2" radius</u>
Boiling plate	.072"	.075"	.072"
Computer model	.050"	.050"	.050"
<u>Distance apart</u>			
Boiling plate	.364"	.362"	.367"
Computer model	.400"	.400"	.400"

Figure 14 compares the boiling surface flux (BOIL) and the flux calculated by taking temperatures within the plate (MEASRD). Hence,

Figure 13. Temperature Distribution Inside of Computer Model of Boiling Plate

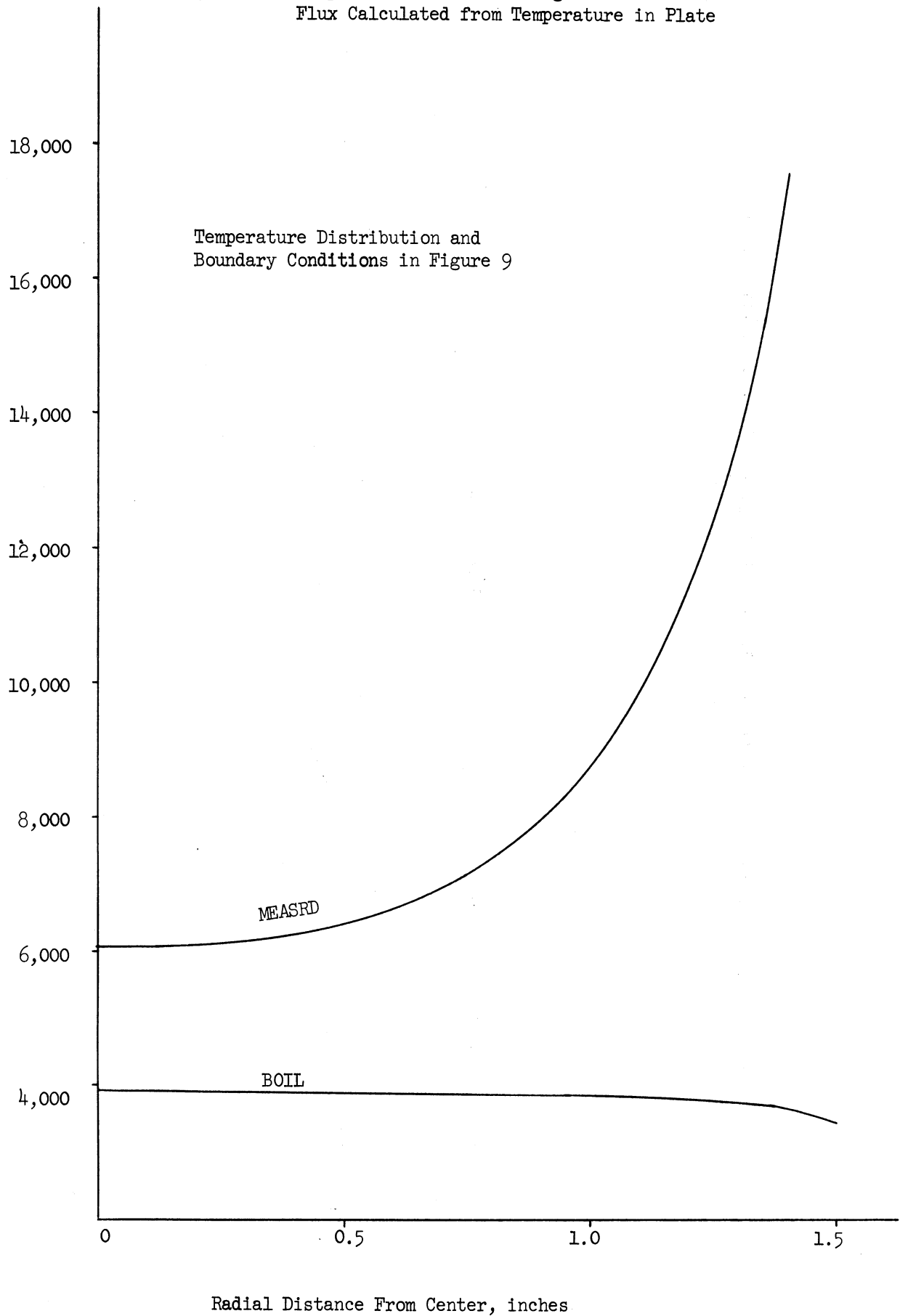
Assumed Temperature of Said Liquid = 691°F



Assumed Temperature Distribution at Bottom of Plate



Figure 14. Comparison Between Boiling Surface Flux and Flux Calculated from Temperature in Plate



thermocouples in the plate would give a high estimate for the value of the flux actually occurring at the boiling surface. This measured flux for the set of conditions in Figure 13 would be in error by 55% at the center of the plate and would increase to over 6 times the boiling surface flux at the junction of the boiling plate and the tube wall.

This information provided by the computer model can be used to estimate the error involved in the experimental temperature measurements in the boiling plate. One method is to use the ratio MEASRD/BOIL to correct the calculated fluxes.

	<u>1/2" radius</u>	<u>1" radius</u>
MEASRD	6,453	8,797
RATIO = MEASRD/BOIL (Figure 10)	1.6545	2.2974
Experimental q/A	6,480	8,860
Corrected q/A (q/A/RATIO)	3,940	3,860

Another method is to use directly the boiling flux based on the assumed boiling coefficient and the surface temperatures calculated by the computer.

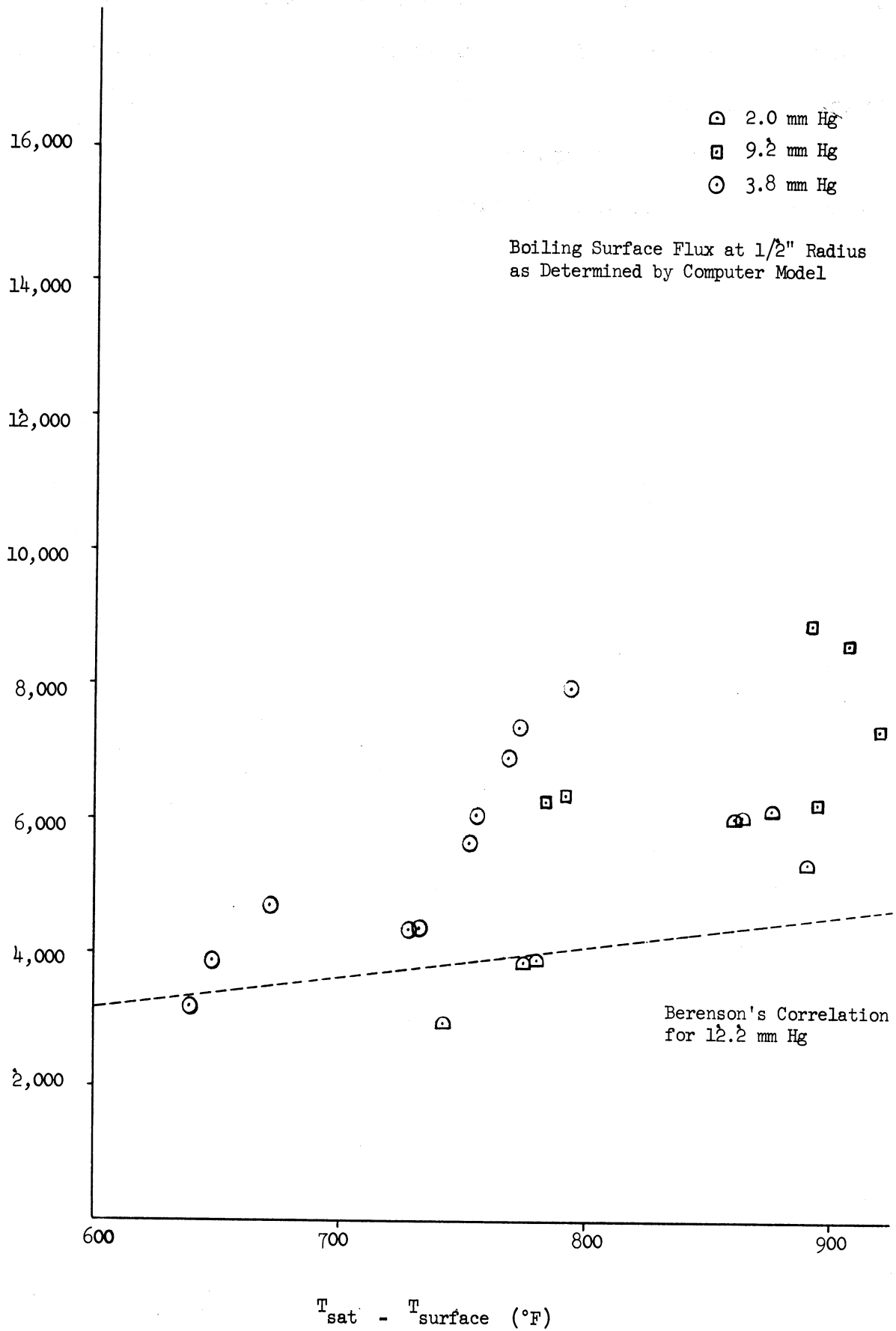
	<u>1/2"</u>	<u>1"</u>
T <sub>surface</sub> , °F	1471.1	1456.8
T <sub>sat</sub> , °F	691	691
h (assumed), BTU/(hr.)(sq.ft)(°F)	5.0	5.0
q/A, BTU/(hr.)(sq. ft)	3900	3829

The difference is small and the last method will be utilized for handling the data. Figure 15 and table 1 show the data for all the cases in which the type of computer analysis discussed above could be carried out. These cases represent approximately one-third of the data actually taken. The

TABLE 1  
FILM BOILING OF POTASSIUM

1/2-inch Radius			
$T_{sat}$	h	q/A	$\Delta T_{sat}$
°F	BTU/(hr.)(sq. ft.)(°F)	BTU/(hr.)(sq. ft.)	°F
685	7	6020	860
684	7	6040	863
686	7	6130	875
691	4	2970	742
693	5	3870	774
691	5	3900	780
684	6	5340	890
815	6	4370	728
814	6	4390	732
814	6	3890	648
814	5	3200	639
814	7	4700	671
815	10	7930	793
815	9.5	7340	772
814	7.5	5640	752
814	8	6040	755
814	9	6910	768
749	10	8910	891
744	8	6270	783
742	8	6330	791
742	9.5	8610	906
741	8	7350	919
740	7	626	894

Figure 15. Film Boiling of Potassium



other two-thirds of the data exhibited non-symmetrical temperature distributions in the plate which made it impossible to carry out the analysis. In these cases, one side of the boiling plate was apparently hotter than the opposite side. An attempt will be made in future operation to isolate and avoid the cause of this difficulty.

## FORCED CIRCULATION STUDIES

Robert E. Barry and Robert L. Gahman

Heat transfer and isothermal pressure drop data have been obtained for the two phase flow of potassium over a limited range of vapor temperatures and qualities. The heat flux was varied from 100,000 to 300,000 BTU/(hr.)(sq. ft.); the quality ranged from all liquid to 25% vapor; the flow rate was 200 to 550 pounds per hour; and the vapor temperature ranged from 1400° to 1500°F. The data is being reduced at this time and will be presented in a future report.

### Loop Operation

Immediately after beginning operations on May 11, the original pump, a MSAR Style II Electromagnetic Pump with a .065-inch pumping width, became plugged. Problems had been encountered with this pump before and it was replaced with a Style IV pump which has a .183-inch pumping width. It was expected that this would alleviate the problems associated with the repeated plugging of the pump. During later operation it was necessary to cut out a filter by-pass valve directly upstream of the pump. At this time the pump was visually inspected and there was no evidence of plugging in the Style IV pump.

After the pump was replaced, operation was again resumed. During the charging operation the supply valve froze open and it was necessary to dump the loop and replace the valve. Inspection of the valve indicated that the stem had galled in the yoke. This supply valve, a Hoke HY477A, had never been used above temperatures of 300°F. However,

an identical valve had been operated satisfactorily over 200 hours at temperatures over 1300°F. The supply valve was replaced with a Hoke HY 477B with a Stellite seat.

After this repair was completed the loop was again charged and operated in the two phase flow regime for 15 hours. Heat was transferred to the two phase potassium in the test section by sodium condensing on the outside of the vertical Haynes-25 tube. Due to time lags, primarily resulting from liquid holdup in the hot well, an excessive amount of heat was removed in the condenser and sub-cooler. It should be noted that this was the first time that the condenser and subcooler were needed to control the loop temperature. In prior operations heat input had never been great enough to require operation of the louvers and blowers. The delayed response of the system to the excessive heat removal caused the inlet temperature of potassium to the preheaters to drop to 600°F. At this temperature occasional restrictions in the flow occurred apparently due to the precipitation of either oxides or corrosion products. Similar behavior was later experienced with fluid temperatures of 900°F. These plugs were successfully dislodged by surging the pump. The loop was also dumped hot upon shutdown to carry a maximum amount of contaminants to the supply tank where they could be precipitated.

Prior to dumping the system 38 data points were obtained with the loop operating in two phase flow. Operation was continuous for a period of five days during which time potassium temperatures were maintained between 1400°F and 1500°F. Quality ranged up to 25% and threefold ranges of flow rate (200 to 550 pounds per hour) and heat flux

(100,00 - 300,00 BTU/(hr.)(sq. ft.) were obtained. Overall heat transfer coefficient, void fraction and pressure drop was determined for each steady state setting. The latter two determinations will be discussed in the following section.

Overall heat transfer coefficients were determined by measuring the sodium vapor temperature on the condensing side of the tube and the potassium temperature at the exit of the 2-inch test section. A second measurement of the potassium temperature was made just downstream from the first but after the fluid made a 90 degree turn. The turn should have produced some mixing and restored equilibrium conditions between liquid and vapor if they had not existed in the test section. Both potassium thermocouples agreed within the limits of error associated with their operation. This concurrence suggested that the non-equilibrium conditions experienced by Chen at Brookhaven (3) were not affecting the potassium temperatures in the test section.

Heat fluxes were determined from power settings on the sodium boiler in combination with heat loss calibrations for the sodium system. From these measurements the overall coefficient could be calculated. Earlier determinations of the condensing coefficient on this system and a knowledge of the thermal resistance of the Haynes wall should permit a calculation of the two phase potassium heat transfer coefficient. These results will be reported as soon as data processing is complete.

During the period over which the above data was obtained, several of the preheater connections burned out reducing preheat capacity to almost half of capacity. The failures occurred at the junctions where



the lead wire is connected to the heating element. These repairs are being made at the present time. Following completion of these changes operation will again commence and additional data obtained.

### Void Fraction Studies

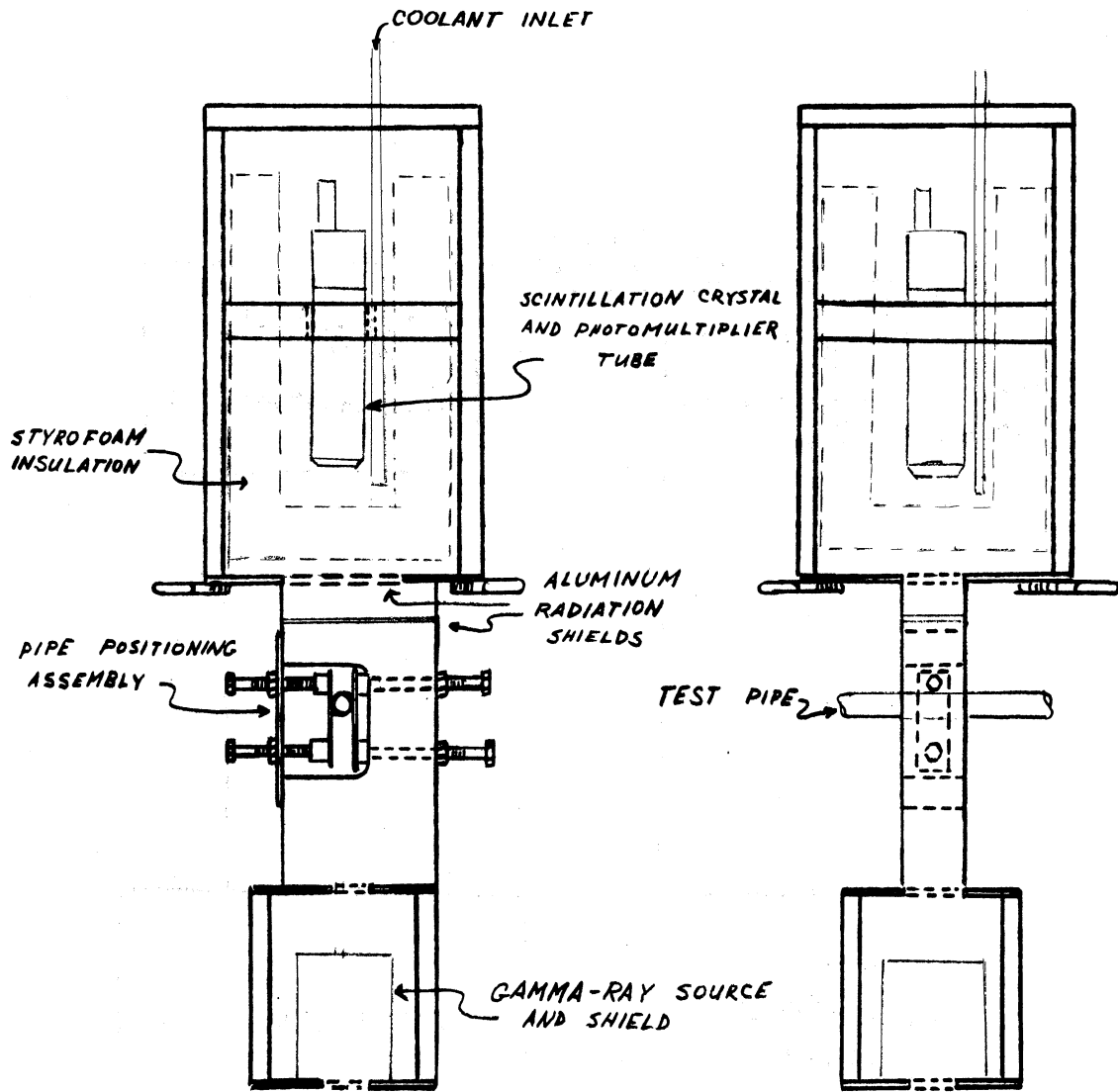
The current contract includes specifically the measurement of pressure drop and void fraction for two phase flow. Although both had been studied earlier with potassium (8% sodium), it was felt that certain modifications to the radiation attenuation apparatus could reduce scatter. During loop shutdown, several modifications were made which are shown in Figure 16. Both source, Tm 170, and detector are fixed on the same assembly which clamps onto the pressure drop test pipe to maintain an accurate position. In addition, a frostless cooling system using carbon dioxide generated by dry ice was installed. The cold gas passed across the crystal back out of the Styrofoam container and out through a loose fit in the thermal radiation shields.

Originally a Tracerlab SC-18 Superscaler was used as both a high voltage supply and counter. It became evident that the high voltage supplied by this instrument was not stable enough to provide good results. In addition, problems with the preset time switch made use of another scaler mandatory. Also the discrimination level provided by the instrument was not sufficient to control the noise level.

Equipment was obtained to form the setup as shown in Figure 17. The scintillation device is a Harshaw Integral Line Assembly Model 4S4. The crystal was NaI thallium activated and was 1-inch in diameter by 1-inch thick. The scaler was a Radiation Counter Laboratories Decade Scaler Model 10D. A Baird Atomic Regulated High Voltage Supply Model

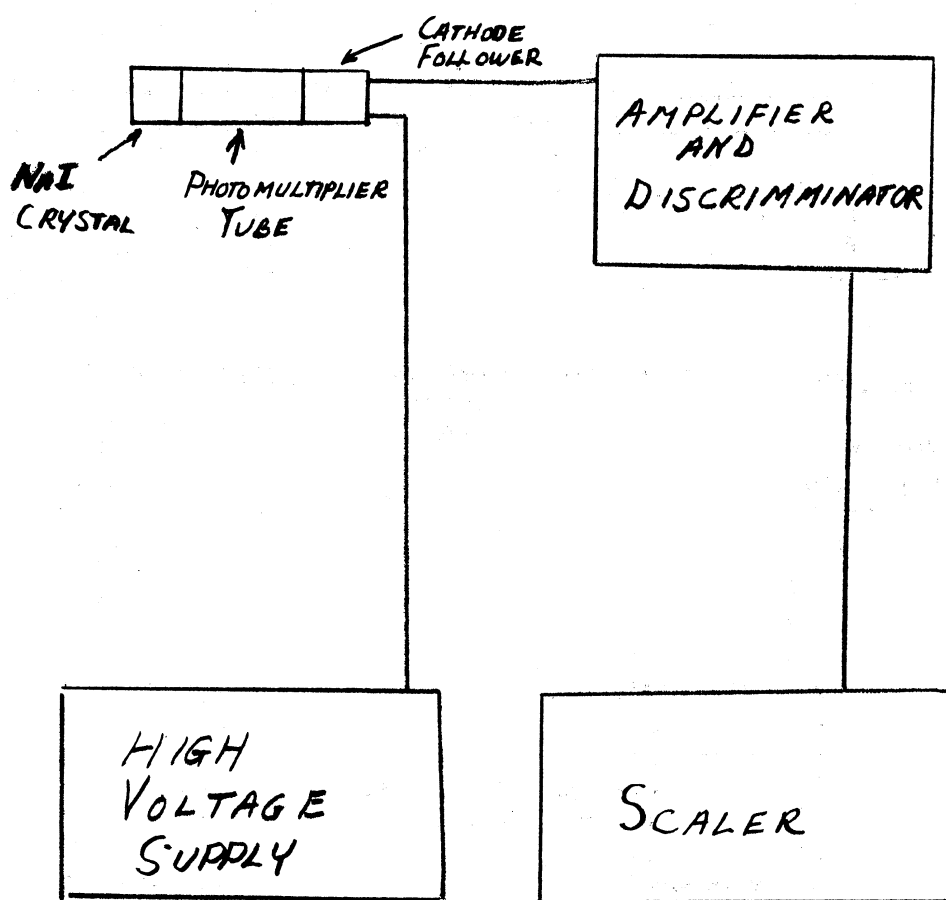
# GAMMA-RAY SOURCE AND SCINTILLATION CRYSTAL HOLDER

FIGURE 16



## VOID FRACTION INSTRUMENTATION

FIGURE 17



316 eliminated instabilities in the high voltage. To provide the necessary level of discrimination of noise and energy a Baird Atomic University Series Model 212 amplifier was used.

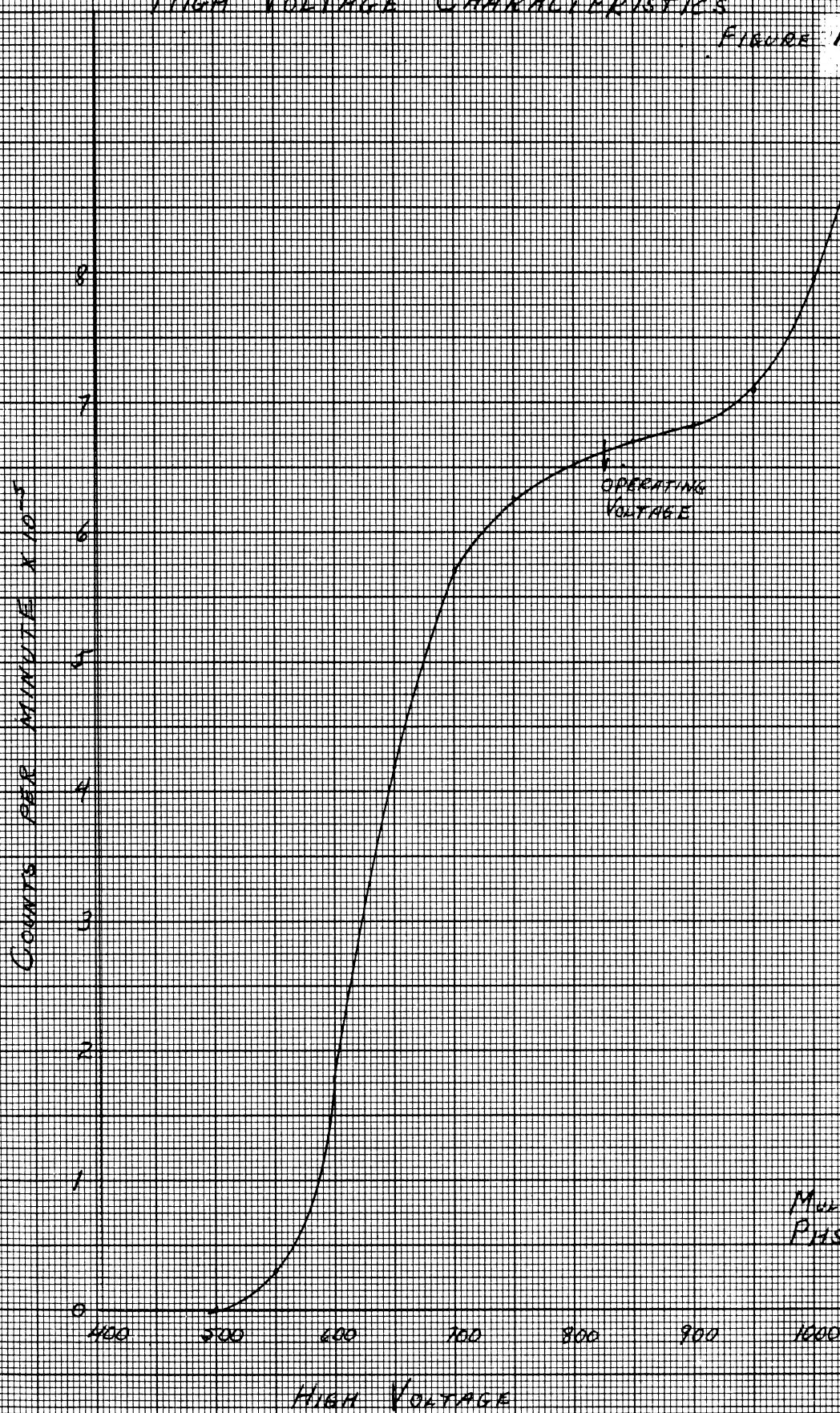
With this instrumentation it was possible to determine the optimum operating voltage for the crystal. As seen from Figure 18, 850 volts was used.

Also a differential pulse height, or energy, spectrum of the Tm 170 source was obtained. Figure 19 shows the spectrum. On the basis of this, the discrimination level was set on the top of the .084 Mev. gamma peak of the Tm 170. This technique brought the background level down to where it was negligible as compared to the Tm 170 count level.

Difficulty in the operation of the void fraction apparatus arose in the use of the Styrofoam insulation. It shrunk and warped out of shape allowing the lead shot to drop and the temperature of the crystal to rise uncontrollably. The cooling system was able to keep the crystal at about 80° while the pipe rose to 1500° while the Styrofoam jacket was reasonably in place. Steps are being taken to correct this type of malfunction.

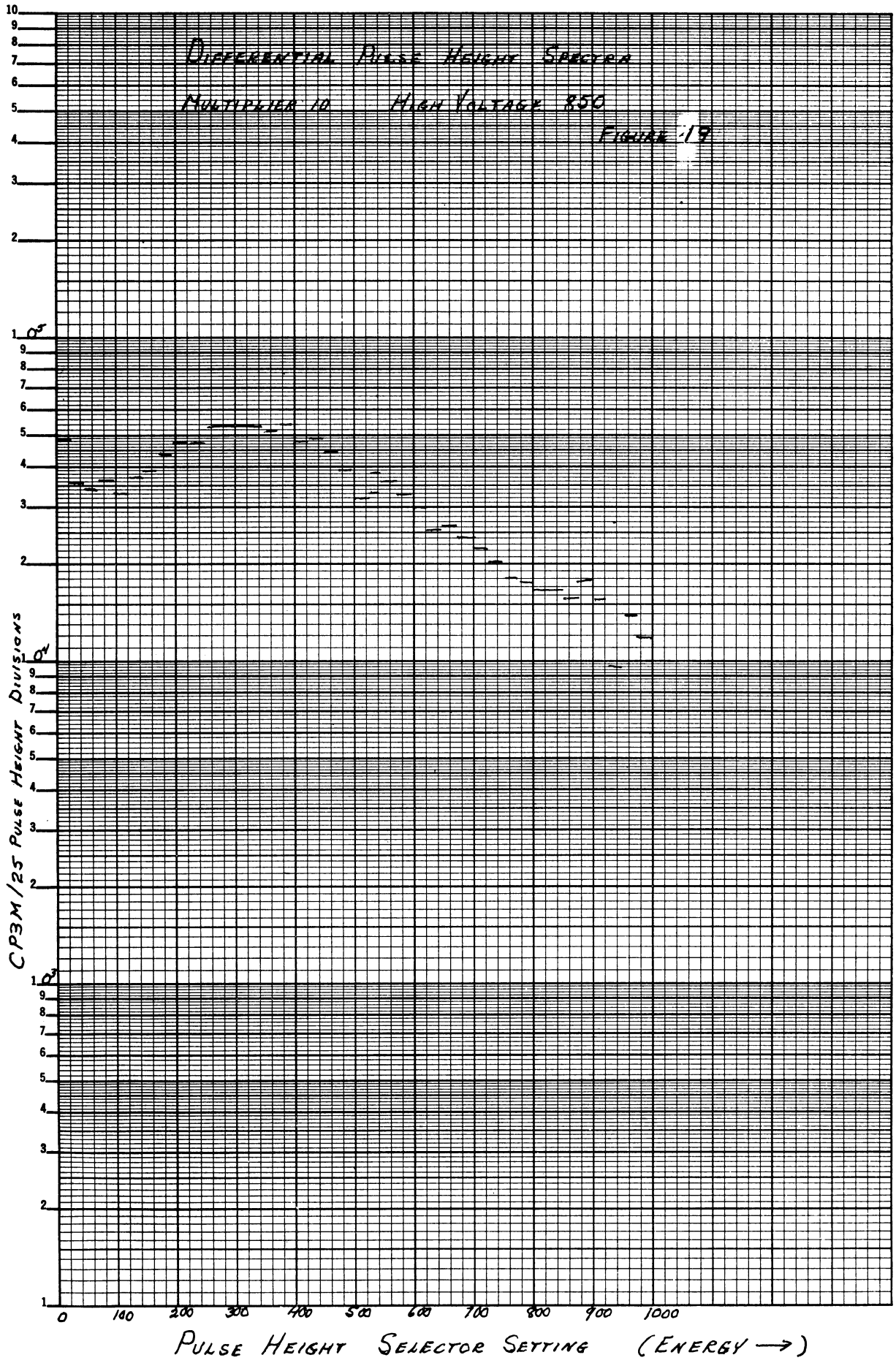
# HIGH VOLTAGE CHARACTERISTICS

FIGURE 18



MULT. 1  
PMS 600

HIGH VOLTAGE



## THE CONDENSATION OF SODIUM AT HIGH HEAT FLUXES

Robert E. Barry

Sodium was condensed on the outside of a vertical,  $1/2$ -inch diameter tube, internally cooled by a flow of liquid potassium at heat fluxes of from 215,000 to 583,000 BTU/(hr.)(sq. ft.). The vapor temperature was varied from 1240°F to 1525°F providing a five-fold variation in the vapor density. The condensing heat transfer coefficient was obtained from a measurement of the overall heat transfer coefficient in conjunction with calculated values of the resistance of the tube wall and the coolant.

The sodium condensing heat transfer coefficient was found to be a constant over the range of experimental conditions having a value of  $10,800 \pm 3300$  BTU(hr.)(sq. ft.)(°F). This value agrees with previous data taken at much lower heat fluxes and represents 8 - 10 percent of the theoretical value. The data were also examined from the standpoint of the kinetic theory of condensation, but since the mass rate of condensation was found to be independent of the vapor pressure, the use of this theory to explain the condensation of liquid metals at moderate temperatures and pressures does not appear to be justified.

## REFERENCES

1. Balzhiser, R. E., et al. "Investigation of Liquid Metal Boiling Heat Transfer", 6th Quarterly Progress Report, 05750-19-P, The University of Michigan, February 1965.
2. Balzhiser, R. E., et al. "Investigation of Liquid Metal Boiling Heat Transfer," 5th Quarterly Progress Report, 05750-16-P, The University of Michigan, September 1964.
3. Chen, John C. Brookhaven National Laboratory, Upton, New York, Private Communication.





3 9015 02229 2612